JOURNAL OF MATERIALS SCIENCE 22 (1987) 4177–4180

The structure and electrical conductivity of Mn–Cd ferrite

S. A. MAZEN, A. E. ABD-EL-RAHIEM
Faculty of Science, Zagazig University, Zagazig, Egypt
B. A. SABRAH
Faculty of Education, Cairo University, Fayoum, Egypt

Polycrystalline samples of mixed ferrite $Mn_{1-x}Cd_xFe_2O_4$, where x = 0, 0.2, 0.4, 0.6 and 0.8, were studied by X-ray analysis and d.c. electrical conductivity. It was found that the calculated lattice parameter (a_0) increases from 0.855 to 0.861 nm according to increases in x from 0 to 0.8. The apparent density and theoretical density exhibit the same behaviour. It was also found that the activation energy of the conduction mechanism and log $\varrho_{27^\circ C}$ increase with increasing cadmium content, which affect the exchange interaction mechanism in tetrahedral (A) sites and octahedral (B) sites.

1. Introduction

Manganese–zinc ferrite and nickel–zinc ferrite are still by far the most imortant ferrites for high-permeability and low-loss applications [1]. By varying the ratio of zinc to manganese or nickel, or by other means, both types of ferrite may be made in a variety of grades, each grade having properties that suit it to a particular class of application. In addition to their use in magnetic applications, ferrites can also be used as thermistors, but sometimes the resistivity is very low [2]. Therefore, the control of resistivity in ferrites is a serious problem. There are two general approaches to this: (1) controlling firing temperature, and (2) addition of minor constituents to increase or decrease the conductivity. The first point was studied in our previous paper [3], but the aim of this work is to study the effect of cadmium on some physical properties of $MnFe_2O_4$.

2. Experimental details

Polycrystalline samples of mixed ferrite $Mn_{1-x}Cd_xFe_2O_4$ (where x = 0, 0.2, 0.4, 0.6 and 0.8) were prepared by a standard ceramic technique. As seen from our previous work on $MnFe_2O_4$ [3], the homogenization and structure perfection is formed at a sintering temperature of 1150° C. Therefore, this series of Mn–Cd–ferrites was prepared at the same temperature.

Conductivity measurements were carried out over a wide temperature range (from room temperature to 637 K). Measurements during the heating and cooling process were carried out to ensure the absence of any kind of hysteresis. The two-terminal d.c. method and indium-amalgam for contact were used in the measurements. Further details of the preparation and measurements are given elsewhere [3, 4].

The density of the samples was determined using hydrostatic weighing in toluene. A single crystal of germanium was used as a reference material. These measurements were carried out using an electrical balance with a sensitivity of 10^{-4} g.

X-ray diffraction patterns were made of the finest powder samples. A Philips recording diffractometer was used and a Co$K\alpha$ radiation source was applied with an iron filter to obtain the spectrum. A single crystal of silicon was used to calibrate the diffractometer.

3. Results and discussion

3.1. X-ray analysis

X-ray diffraction patterns for the samples are shown in Fig. 1. The X-ray patterns show the reflection planes (2 2 0), (3 1 1), (2 2 2), (4 0 0), (4 2 2), (5 1 1) and (4 4 0). It was observed that the (1 1 1) plane completely disappeared in all samples, but the (2 2 2) and (4 0 0) planes disappeared at high cadmium concentrations. This behaviour agrees with the ASTM cards. Generally, the diffraction data proved that the $Mn_{1-x}Cd_xFe_2O_4$ have been formed in cubic spinel structure. The d-spacings for the recorded peaks are calculated according to Bragg's law. The lattice parameter (a nm) can be calculated directly using the following relation:

$$a = d_{(hkl)}(h^2 + K^2 + L^2)^{1/2} \quad (1)$$

where h, K and L are the indices of the mentioned planes. The measured lattice parameters are plotted against the function $F(\theta) = [1/2\ (\cos^2\theta/\sin\theta) + (\cos^2\theta/\theta)]$ in Fig. 2; a straight line resulted. The value of a_0 (the true value of a) can be found by extrapolating this line to $F(\theta) = 0$ as $\theta \to 90°$. The lattice parameters, a_0, as a function of composition are tabulated in Table I. Fig. 3a shows the relation between the composition and lattice parameter, a_0. From this figure, one can clearly see that the lattice parameter increases with increasing cadmium content. This observation may be accounted for the replacement of manganese by cadmium ions, because the ionic radius

0022–2461/87 $03.00 + .12

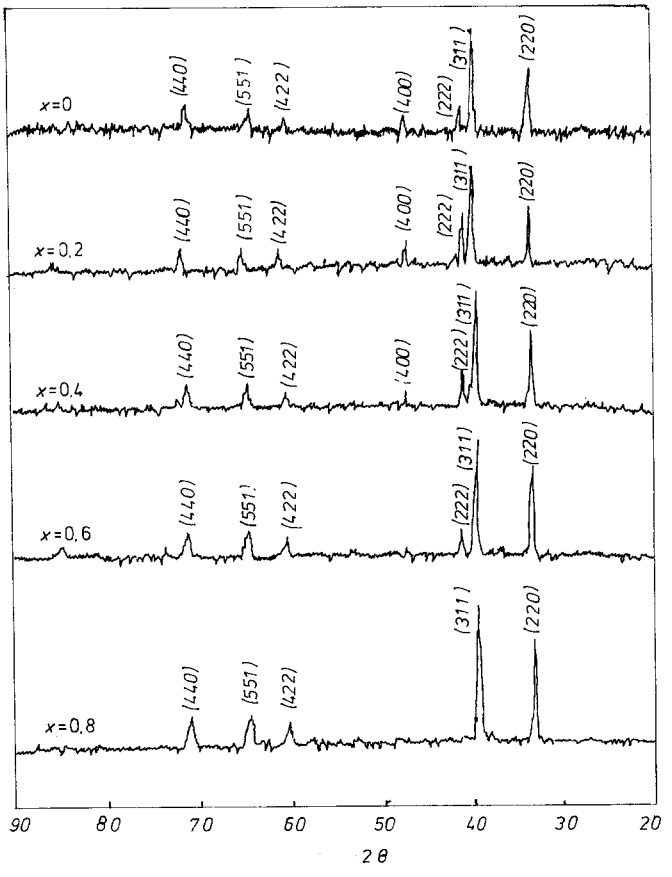

Figure 1 X-ray diffraction pattern of $Mn_{1-x}Cd_xFe_2O_4$ ferrite.

of Mn^{2+} (0.052 nm) is smaller than that of Cd^{2+} (0.099 nm) [5].

It is known that there is a correlation between the ionic radius and the lattice constant [6]. Pascard *et al.* [7] found that the distance between the magnetic ions on the tetrahedral sites (i.e. the lattice constant) increases with the introduction of larger ions for $Ni_{1-x}Zn_xFe_2O_4$ and $Ni_{1-x}Cd_xFe_2O_4$. In this work, the relation between the tetrahedral ionic radii and the lattice parameters of $Mn_{1-x}Cd_xFe_2O_4$ has been studied. It is well known that the Cd^{2+} ions occupy the tetrahedral position (A-sites) only [8]. Starting from the basic $MnFe_2O_4$, non-magnetic Cd^{2+} ions are substituted to replace Mn^{2+} ions in the A-sites and Fe^{3+} ions, which in turn move into octahedral sites

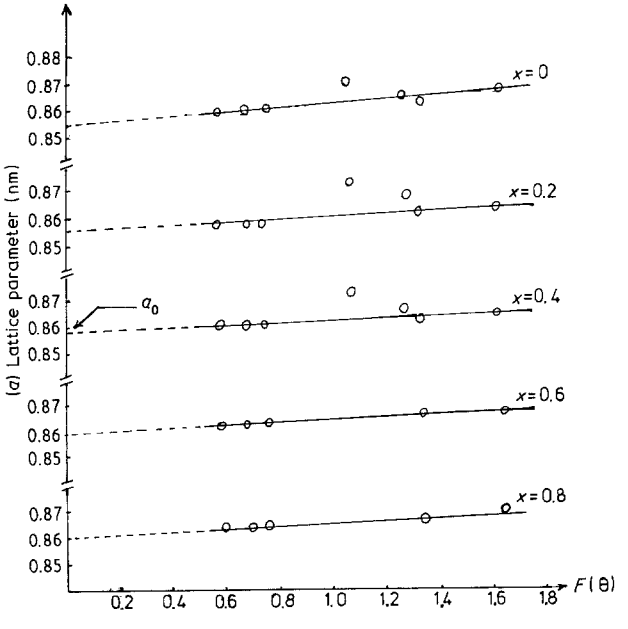

Figure 2 Relation between the lattice parameter and $F(\theta) = 1/2[(\cos^2\theta/\sin\theta) + (\cos^2\theta/\theta)]$ for different compositions of Mn–Cd ferrite.

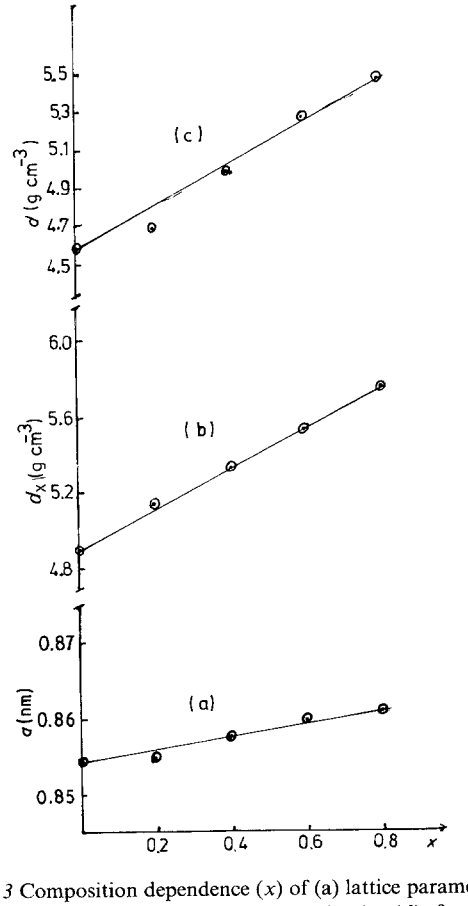

Figure 3 Composition dependence (x) of (a) lattice parameter (a_0), (b) X-ray density (d_x), and (c) apparent density (d), for Mn–Cd ferrite.

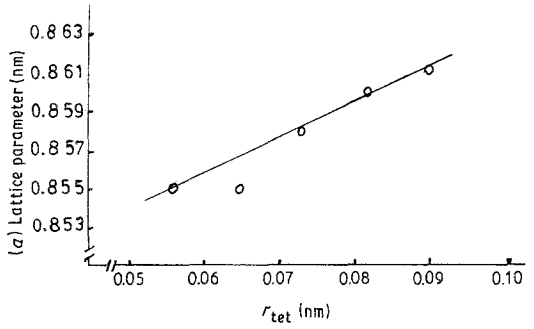

Figure 4 Tetrahedral ionic radius ($r_{tet.}$) plotted against lattice parameter (a_0) for Mn–Cd ferrite.

(B-sites). For a given composition (x), the mean ionic radius for a molecule on the A-sites is defined as [9]

$$r_{tet.\ ion} = (1 - x)r_{tet.\ Fe^{3+}} + (x)r_{tet.\ Me^{2+}} \quad (3)$$

where Me^{2+} denotes the substituted divalent metal. By using this formula, the tetrahedral ionic radius for each composition was computed and tabulated in Table I. Plots of tetragonal ionic radius ($r_{tet.}$) against the lattice parameter (a_0) of $Mn_{1-x}Cd_xFe_2O_4$ are shown in Fig. 4. Starting with $MnFe_2O_4$ when cadmium is doped, the lattice parameter is found to increase with increasing cadmium content, because Cd^{2+} with a larger ionic radius, replaces Mn^{2+}, which has a smaller ionic radius, on the tetrahedral sites (A-sites).

As the lattice parameter (a_0) was calculated precisely, the X-ray density (theoretical density), d_X, was

TABLE I

Composition (x)	a_0 (nm)	$r_{tet.}$ (nm)	dx (g cm^{-3})	d (g cm^{-3})
0	0.855	0.056	4.90	4.50
0.2	0.855	0.065	5.15	4.70
0.4	0.858	0.073	5.34	5.00
0.6	0.860	0.082	5.54	5.28
0.8	0.861	0.090	5.76	5.41

The error in d_0 (nm) does not exceed 0.2%.

calculated as follows

$$d_X = 8M/Na_0^3 \text{ g cm}^{-3} \quad (4)$$

where M is the molecular weight, N is Avogadro's number, 8 is the number of molecules per unit cell. The apparent density (d g cm^{-3}) was also measured. The dependence of density (d) and X-ray density (d_X) upon cadmium concentration is tabulated in Table I, and represented in Figs 3b and c. It is seen that the X-ray density increases linearly with increasing cadmium content, where the atomic weight of cadmium (112.4) is higher than that of manganese (54.94). In addition the apparent density (d g cm^{-3}) of the same compositions nearly reflects the same general behaviour of the theoretical density (d_X).

3.2. D.c. electrical conductivity

The d.c. electrical conductivity of the Mn–Cd ferrite has been investigated throughout this work. Fig. 5 shows the observed variation of log σ with T^{-1} for $Mn_{1-x}Cd_xFe_2O_4$. As expected for all semiconduc-

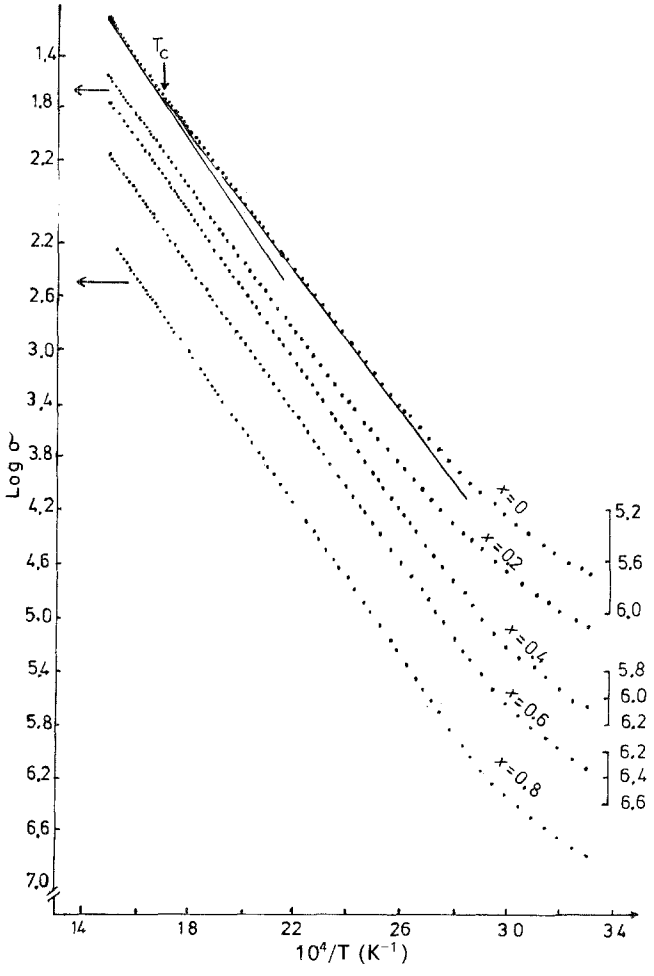

Figure 5 The observed variation of log σ against T^{-1} for various samples of Mn–Cd ferrite.

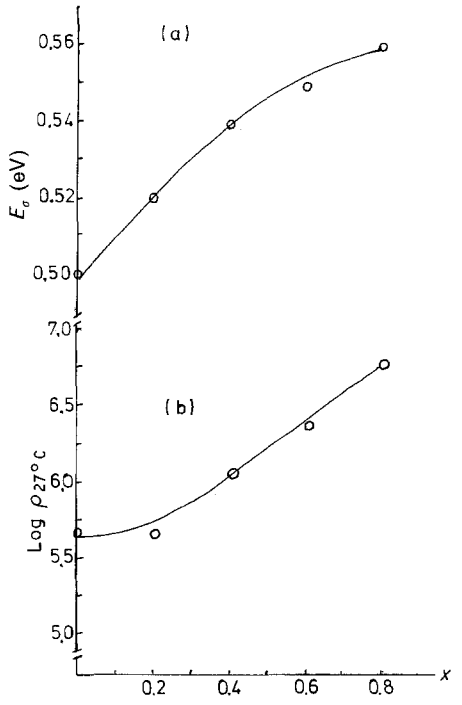

Figure 6 The variation of (a) the activation energy, E, and (b) the log $\varrho_{27°C}$ with composition, x.

tors, the conductivity of the ferrites was observed to increase with rising temperature. The conductivity (σ) at an absolute temperature, T, is known to be given by $\sigma = \sigma_0 \exp(-E_\sigma/KT)$. In this paper we shall discuss the effect of cadmium on the conduction mechanism of $MnFe_2O_4$. The behaviour of $MnFe_2O_4$ (i.e., $x = 0$) at T_C (Curie point) was discussed in detail in the previous work [3] to which the reader is referred. The behaviour of activation energy E_σ(eV) for various samples with composition is represented in Fig. 6a. A similar behaviour has also been observed for the relation between $\log \sigma_{27°C}$ and composition (x) as shown in Fig. 6b.

The experimentally observed variation of d.c. electrical conductivity with cadmium content is thus qualitatively explained by the assumption that as the cadmium content increases the relative number of ferric ions on the A-sites diminishes. This causes the (A–A) and (A–B) exchange interactions to be reduced with the increasing cadmium concentration. Therefore, ferrites containing an appreciable amount of cadmium are characterized by a fairly strong (B–B) exchange interaction [2]. This would greatly affect the activation energy needed for the transfer of the electrons between Fe^{2+} and Fe^{3+} ($Fe^{2+} \rightleftharpoons Fe^{3+}$) and consequently the conductivity process. The replacement of manganese ions by cadmium ions in A-sites may lead to the following processes: (i) the introduction of manganese ions in the B-sublattice as Mn^{3+} [10] would obstruct the electron hopping between the iron ions by blocking the $Fe^{2+} \rightarrow Fe^{3+}$ exchange; (ii) if the Fe^{3+} ions at the B-sites are converted to Fe^{2+} ions for charge compensation, the conduction due to electron hopping is modified because of a decrease in the number of Fe^{3+} ions and an equal increase in the number of Fe^{2+} ions in the B-sublattice. Process (i) increases the resistivity of the sample and Process (ii) may increase or decrease the resistivity, but the probability of an increase is greater than a decrease. Moreover the replacement of manganese ions ($4s^2 3d^5$) by cadmium ions ($4s^2 3d^{10}$) whose d-electrons do not participate in the conduction process but limit the degree of conduction [4]. On the other hand, the electron hopping between B–A sites is less probable compared to that for B–B hopping, because the distance between two metal ions placed in B-sites is smaller than that if they were placed one in a B-site and the other in an A-site [2, 8]. Thus the hopping probability depends upon the separation between the ions involved and the activation energy of the conduction process [11].

References

1. D. POLDER, *Proc. Inst. Electron Eng.* **97**(II) (1950) 246.
2. K. J. STANDLEY, "Oxide Magnetic Materials" (Clarendon, Oxford, 1972).
3. S. A. MAZEN and B. A. SABRAH, *Thermochim. Acta.* **105** (1986) 1.
4. S. A. MAZEN, B. A. SABRAH, A. A. GHANI and A. H. ASHOUR, *J. Mater. Sci. Lett.* **4** (1985) 479.
5. N. AKHMETOR, "Inorganic Chemistry" (Mir, Moscow, 1973).
6. F. H. S. VEMAAS and E. R. SCHMIDT, *Beitr. Mineral, Petrogra* **6** (1959) 219.
7. H. PASCARD, A. GLOBUS and V. CABON, *J. Phys. (Paris) Collog.* **38**, C1 (1977) 163.
8. S. CHIKAZAMI, "Physics of Magnetism" (Wiley, New York, London, Sydney, 1964).
9. P. VENUGOPAL REDDY and T. SESHEGIRIRAO, *J. Less-Common Metals* **75** (1980) 255.
10. N. RELLESCU and E. CUCIUREANU, *Phys. Status Solidi A* **3** (1970) 873.
11. K. H. RAO, S. B. RAJU, K. AGGARWAL and R. G. MENDIRATTA, *J. Appl. Phys.* **52** (1981) 1376.

Received 12 February
and accepted 29 April 1987